ENVIRONMENTAL RESEARCH
LETTERS

OPEN ACCESS

RECEIVED
8 April 2025

REVISED
19 July 2025

ACCEPTED FOR PUBLICATION
22 July 2025

PUBLISHED
11 September 2025

LETTER

Intensifying heat extremes in China attributed to rising greenhouse gases and declining aerosols since the 2010s

Aili Zou[1,2], Yang Yang[1,2,*], Hailong Wang[3], Pinya Wang[1,2], Ke Li[1,2], Yuanjian Yang[4], Chao Liu[4], Jiandong Wang[4] and Hong Liao[1,2]

[1] State Key Laboratory of Climate System Prediction and Risk Management/Jiangsu Key Laboratory of Atmospheric Environment Monitoring and Pollution Control/Jiangsu Collaborative Innovation Center of Atmospheric Environment and Equipment Technology/Joint International Research Laboratory of Climate and Environment Change, Nanjing University of Information Science and Technology, Nanjing, Jiangsu, People's Republic of China
[2] School of Environmental Science and Engineering, Nanjing University of Information Science and Technology, Nanjing, Jiangsu, People's Republic of China
[3] Atmospheric, Climate, and Earth Sciences Division, Pacific Northwest National Laboratory, Richland, WA, United States of America
[4] School of Atmospheric Physics, Nanjing University of Information Science and Technology, Nanjing, Jiangsu, People's Republic of China
[*] Author to whom any correspondence should be addressed.

E-mail: yang.yang@nuist.edu.cn

Keywords: heat extreme, heatwave, greenhouse gases, aerosols

Supplementary material for this article is available online

Abstract

Rising temperatures have increased the frequency, duration, and intensity of extreme temperature events over China in recent decades. The upward trends in heat extremes in China in the warm season (May–September) and their relationships with changes in aerosols and greenhouse gases are investigated using observations, reanalysis data and model results. Significant increasing trends in China are observed in daily maximum temperatures (TXx), heatwave frequency, and heatwave mean duration during 2011–2023, with increasing rates of 0.70 °C/decade, 3.77 d/decade and 0.31 d/event/decade, respectively. This study shows that 43 ± 3% of the TXx increases in China are attributed to the rising CO_2 concentrations. Aerosol optical depth in China decreased at a rate of 0.054 per decade from 2011 to 2023 due to significant air quality improvements. The weakened aerosol cooling effect due to declining aerosols contributes 27 ± 3% to the observed TXx trend. In eastern China, where aerosol reductions were most significant, aerosol reduction even accounts for 79 ± 10% of the TXx increasing trend. The intensifying heat waves attributed to GHGs and aerosols are in accordance with the increasing extreme high temperatures. The results highlight the significant impacts of rising GHGs and decreasing aerosols on heat extreme events over China in recent years, emphasizing the need of considering both GHGs and aerosols to address the issue of intensification of heat extremes in a warming future.

1. Introduction

Due to increasing concentrations of greenhouse gases (GHGs) from human activities, warming occurs in many regions of the world, with the rise of present-day global mean surface air temperature by 1.1 °C compared to pre-industrial levels (IPCC 2021). The increases in temperature have induced unprecedented changes in the Earth system, causing rapid increases in the frequency, duration, and intensity of extreme heatwaves since the 1950s (Perkins-Kirkpatrick and Lewis 2020). Heatwave is a specific type of extreme high temperature event, characterized by prolonged periods of excessive heat, which have been extensively applied in assessing both historical and future changes in high temperatures (e.g. Bartusek *et al* 2022, Wang *et al* 2023a). Heatwaves represent one of the most severe climate threats, with far-reaching impacts on human health, environment, and infrastructure (Singh *et al* 2021, Sharma *et al* 2022). For example, in late June 2021, an unprecedented heatwave in the Pacific Northwest region of Canada and the United States broke the local temperature record with temperatures reaching 49.6 °C, which led to catastrophic consequences, including hundreds of deaths, marine species die-offs, reduced agricultural yields, flooding from rapid snowmelt, and a significant rise in wildfires (White *et al* 2023).

Many regions in China have observed that the frequency and intensity of heatwave events and their associated compound events in China have doubled since 1960 (Chen *et al* 2019, Luo *et al* 2020b, Wang and Yan 2021, Wang *et al* 2023b). Furthermore, persistent climate warming is anticipated to result in a substantial increase in high temperature extremes. It is projected that heatwaves would become increasingly frequent and intense under various future scenarios, according to the Coupled Model Intercomparison Project phase 6 (CMIP6) multi-model ensemble projections and machine learning methods (Zhang *et al* 2024).

Variations in GHGs and aerosols exert crucial impacts on heat extreme events. Most previous studies have primarily emphasized the role of increasing greenhouse gases (GHGs), particularly CO_2, in driving extreme temperature trends (e.g. Angélil *et al* 2014, Xu *et al* 2018). During the 20th century, the increase in anthropogenic aerosols acted to mask part of the GHGs-induced warming, especially in polluted regions like East Asia and India, leading to an underestimation of GHGs effects on extreme temperatures (Sonali and Nagesh Kumar 2016, Dileepkumar *et al* 2018, Seong *et al* 2021, Shilin *et al* 2024). Xu *et al* (2023) attributed the intensity, frequency, and duration of extreme temperatures in China during 1960–2020 in both observations and CMIP6 simulations to GHGs, aerosols, natural forcing, and land use/cover change, and found that GHGs were the main driver of extreme high temperatures changes in China, with aerosol forcing change contributing a cooling effect that partially offset the warming effect of GHGs. Zhao *et al* (2019) utilized the Community Earth System Model (CESM) Large Ensemble experiments to distinguish the effects of GHGs and aerosols on future global heatwaves under the Representative Concentration Pathway 8.5 scenario, showing that while more severe heatwaves came mainly from GHGs increases, aerosol reductions could have also contributed considerably over the Northern Hemisphere. Yang *et al* (2023) investigated the climatic impacts of aerosol reductions resulting from clean air actions in China under a carbon neutrality scenario and found that the reductions in aerosols can lead to a rise in surface temperatures in eastern China by 0.2 °C–0.5 °C in 2030 and exceeding 0.5 °C in 2060 relative to 2015. Wang *et al* (2023a) isolated the respective roles of GHGs, aerosols and tropospheric ozone in driving climate change and extreme weather events under the future carbon-neutral scenario based on the CESM model simulations. They found that aerosol reductions would lead to a significant warming across the globe and a notable rise in extreme heat events, characterized by higher frequency and greater intensity, with the contributions from aerosol reductions being larger than those due to the changes in GHGs and tropospheric ozone in a carbon-neutral future.

The scientific focus of this study is to explore the trends of intensity, frequency, and duration of extreme high temperatures in China during 2011–2023 and the underlying mechanisms. The selection of this time period is motivated by the significant policy-driven reductions in emissions of aerosols and precursors in China since the 2010s, which mark a turning point from previously stable or increasing aerosol levels to a sharp decline in aerosol optical depth (AOD) across China (Benas *et al* 2020, de Leeuw *et al* 2023, Kong *et al* 2025, Zou *et al* 2025). Using observations, reanalysis data and CMIP6 multi-model simulations, this study analyzes the overall trends of extreme high temperatures in China during the warm season (May–September) from both temporal and spatial perspectives and quantifies the impact of aerosols and GHGs, respectively, on extreme temperature events.

2. Data and methods

2.1. Observations and reanalysis data

The 2-metre air temperature (T2m) data over 2000–2023 are derived from the ERA5 dataset provided by the European Centre for Medium-Range Weather Forecasts (ECMWF), which has been utilized in many studies (e.g. Li *et al* 2022, Qi *et al* 2024). This study calculates the daily maximum temperature (Tmax) during the warm season (May–September) in China by selecting the highest value from the hourly T2m data points within each day, with a spatial resolution of 0.25° latitude/longitude. AOD data with a spatial resolution of 0.5° latitude × 0.625° longitude for the warm season during 2011–2023 are obtained from the Modern-Era Retrospective analysis for Research and Applications, Version 2 (MERRA-2) reanalysis dataset, managed by the NASA Goddard Earth Sciences (GES) Data and Information Services Center (DISC), which have been widely used in previous studies (e.g. Jia *et al* 2021, Jiang *et al* 2023, Liang *et al* 2024). Monthly average CO_2 concentration collected from the Mauna Loa Observatory from 2011 to 2023, provided by the National Oceanic and Atmospheric Administration (NOAA) Global Monitoring Laboratory (GML), are used in this

Table 1. CMIP6-DAMIP experiments, variables and available models used in this study.

Experiment	Variable	Description	Model
hist-aer	tasmax	Daily maximum near-surface air temperature	CanESM5, BCC-CSM2-MR, FGOALS-g3, MRI-ESM2-0, MIROC6, IPSL-CM6A-LR, ACCESS-ESM1-5, ACCESS-CM2, NorESM2-LM
	od550aer	Aerosol optical thickness at 550 nm	CanESM5, MRI-ESM2-0, MIROC6, IPSL-CM6A-LR, ACCESS-ESM1-5, ACCESS-CM2, NorESM2-LM
	rtmt	Net downward radiative flux at top of atmosphere	MIROC6, IPSL-CM6A-LR, ACCESS-ESM1-5, ACCESS-CM2, NorESM2-LM
	cdnc	Cloud droplet number concentration	MIROC6, NorESM2-LM
hist-CO_2	tasmax	Daily maximum near-surface air temperature	CanESM5, MIROC6
	rtmt	Net downward radiative flux at top of atmosphere	MIROC6

study (Keeling *et al* 1976). In addition, CO_2 concentration observations from the Waliguan station in China (2011–2021) (Ma *et al* 2020), along with daily Tmax observations from the China Meteorological Administration (CMA) during 2011–2023, are also used in this study.

2.2. DAMIP multi-model simulations

CMIP6 involves a large number of climate models, an expanded range of experimental designs, and a vast collection of simulation data (Eyring *et al* 2016). Previous studies have shown that CMIP6 models perform well in simulating AOD and extreme temperature changes in China, although they may slightly overestimate extreme temperatures in some regions (Li *et al* 2021, Zhu *et al* 2021, Ali *et al* 2022). One key activity of CMIP6 is the Detection and Attribution Model Intercomparison Project (DAMIP), which focuses on understanding contributions of various forcing factors to the observed climate change (Gillett *et al* 2016). DAMIP includes experiments that isolate specific drivers. The 'hist-aer' experiment examines the impact of varying anthropogenic aerosol forcing, while other forcings are fixed at their pre-industrial level. Another experiment used in this study is the 'hist-CO_2' experiment, which isolates the effect of changing CO_2 concentrations from other forcings being held constant, with CO_2 used here as a representative of overall GHGs forcing due to its dominant contribution (Dong *et al* 2022). These targeted experiments allow researchers to better understand the individual contributions to climate variability and trends. Table 1 summarizes detailed information of the CMIP6-DAMIP experiments, variables and available models used in this study, including two historical climate experiments ('hist-aer' and 'hist-CO_2') for the period 1950–2020. To ensure consistency and maximize the sample size, we include all available models that provided the necessary outputs covering the 1950–2020 period, using the multi-model ensemble means throughout the study. This study also incorporates CO_2 concentrations data (1950–2014) from the Input4MIPs project, which provides essential input data and external forcings for CMIP6 model simulations.

The CMIP6-DAMIP multi-model simulations are employed to establish the sensitivity of heat extremes to individual external forcings. By applying linear regressions to the CMIP6-DAMIP 'hist-aer' and 'hist-CO_2' experiments over 1950–2020, we obtain the responses of heat extreme indices to changes in AOD and CO_2 concentration, respectively. The long-term period starting from year 1950 helps reduce internal variability and ensures more robust estimates. These derived sensitivities are then combined with observed AOD and CO_2 trends during 2011–2023 to estimate their contributions to recent changes in heat extremes. This approach effectively links model-based responses with real-world observations and follows established detection and attribution practices (Bindoff *et al* 2014, Jones *et al* 2016, Seong *et al* 2022). In addition, we analyze cloud and radiation variables from the 'hist-aer' and 'hist-CO_2' experiments to investigate the physical impacts of aerosol reductions and GHGs increases since the 2010s. This helps to further understand the mechanisms behind the observed changes in heat extremes.

2.3. Extreme high temperature indices

To measure the impacts of anthropogenic forcings on extreme high temperature events, two types of extreme indices, TXx and heatwave-related indices, are derived from Tmax during the warm season in China and analyzed in this study. TXx is defined as the highest Tmax of the year for each grid, as a key metric to represent the intensity of extreme high temperature events (e.g. Wang *et al* 2017, Iles *et al* 2024). Following many previous studies on extreme heat events (e.g. Zhang *et al* 2020, Wang *et al* 2023a), a heatwave event in this study is defined as a period of at least 3 consecutive days with Tmax exceeding the 90th percentile threshold based on the 2000–2023 climatological average at each grid point, in order to establish a reliable status with a sufficiently long dataset. Heatwaves are characterized by the total number of heatwave days and the average duration of heatwave events during the warm season, serving as indicators of the frequency and duration of extreme high temperature events.

3. Results

Figure 1 presents the linear trends of heat extreme indices across China during the warm season from 2011 to 2023, based on ERA5 reanalysis data. TXx shows a general increasing pattern across most of China (figure 1(a)), at a rate up to 0.40 °C per year in parts of the North China Plain and Sichuan Basin, which is validated by CMA station observations (figure S1). Regions with statistically significant warming trends are concentrated primarily in central, southwestern, southern and eastern China. During 2011–2023, more than 98% of days experiencing TXx in China are during heatwaves. The trends in heatwave indices show substantial increases in the frequency and duration of heatwaves in many regions of China (figures 1(b) and (c)), although some areas, particularly in western and northeastern China, exhibit negative trends, possibly due to local climate variability such as changes in soil moisture, cloud cover, precipitation or circulation patterns (e.g. East Asian summer monsoon), which could suppress surface warming or heatwave persistence (Whan *et al* 2015, Wei *et al* 2023, Ye *et al* 2025). Moreover, the relatively short analysis period and lack of observational data in western China may also affect the regional trends. The nationally averaged extreme temperature indices in China during 2011–2023 also present significant increases, with TXx rising at 0.70 °C/decade, heatwave frequency increasing at 3.77 d/decade, and heatwave mean duration increasing at 0.31 d/event/decade (figures 1(d)–(f)). Overall, these trends illustrate a general pattern of increasing maximum temperatures, more frequent heatwave days, and longer heatwave durations in China during the warm season from 2011 to 2023, underscoring the warming climate and the increasing impact of extreme heat events in China over the recent decade.

Over the past few decades, the rising concentrations of GHGs, particularly CO_2, have been a key driver of global warming, which has directly influenced the increasing extreme temperature events (Kweku *et al* 2018, Xu *et al* 2023). Recent studies have emphasized the complex role of aerosols in the global climate system, revealing that reduced emissions of aerosols and precursors have diminished their historical cooling effect, thereby increasing surface air temperatures and decreasing relative humidity, with this relative warming effect potentially surpassing that of GHGs in certain scenarios (Zhao *et al* 2019, Wang *et al* 2023a). Assessing the impacts of changes in GHGs and aerosols on heat extreme trends in China requires an understanding of the relationship between these forcings and heat extreme indices, which can be derived from the CMIP6-DAMIP experiments. In this study, AOD and CO_2 concentrations are employed as metrics to measure variations in aerosols and GHGs, respectively.

Figure 2 illustrates the relationships between extreme temperature indices and the two influencing factors in China during the warm season, based on the CMIP6-DAMIP 'hist-aer' and 'hist-CO_2' experiments from year 1950 to present-day. In the historical period, AOD constantly increased in China during 1950–2009 and then slightly decreased in 2010–2020 (figures 2(a)–(c)), while CO_2 concentrations continued increasing since 1950 (figures 2(d)–(f)). Increased AOD, primarily associated with anthropogenic aerosols, cools the atmosphere by reducing sunlight reaching the surface and modifying cloud properties (Boucher *et al* 2013, Bellouin *et al* 2020). The cooling effect from rising AOD reduces extreme temperatures and heatwave frequency and duration, as evidenced by their negative correlations. This relationship remains robust during the period of declining AOD after 2010 (figures S2). Based on the linear regressions, a unit increase in AOD would reduce TXx by 3.5 ± 0.5 °C, heatwave days by 10.55 ± 1.76 d yr^{-1}, and heatwave mean duration by 2.15 ± 0.43 d/event in China during the warm season, as derived from the CMIP6-DAMIP 'hist-aer' experiment. In contrast, increases in CO_2 concentrations are linked to the rising extreme temperature indices, with an increase of 0.012 ± 0.001 °C in TXx, 0.041 ± 0.008 d yr^{-1} in heatwave days and 0.008 ± 0.002 d/event in heatwave mean duration in China for each 1 ppm rise in CO_2, as simulated in the CMIP6-DAMIP 'hist-CO_2' experiment.

Figure 3 shows the time series of warm season CO_2 concentrations and AOD in China during 2011–2023 from observations and reanalysis data. Both CO_2 concentrations from NOAA GML and at Waliguan station show a monotonic growth, with trends of 24.67 ppm/decade and 24.04 ppm/decade, respectively. According to the sensitivities of heat extreme indices to CO_2 concentrations derived from the 'hist-CO_2' experiment (figures 2(d)–(f)), the CO_2 increase translates into a TXx trend of about 0.3 ± 0.02 °C/decade, heatwave frequency of 1.01 ± 0.20 d/year and heatwave mean duration

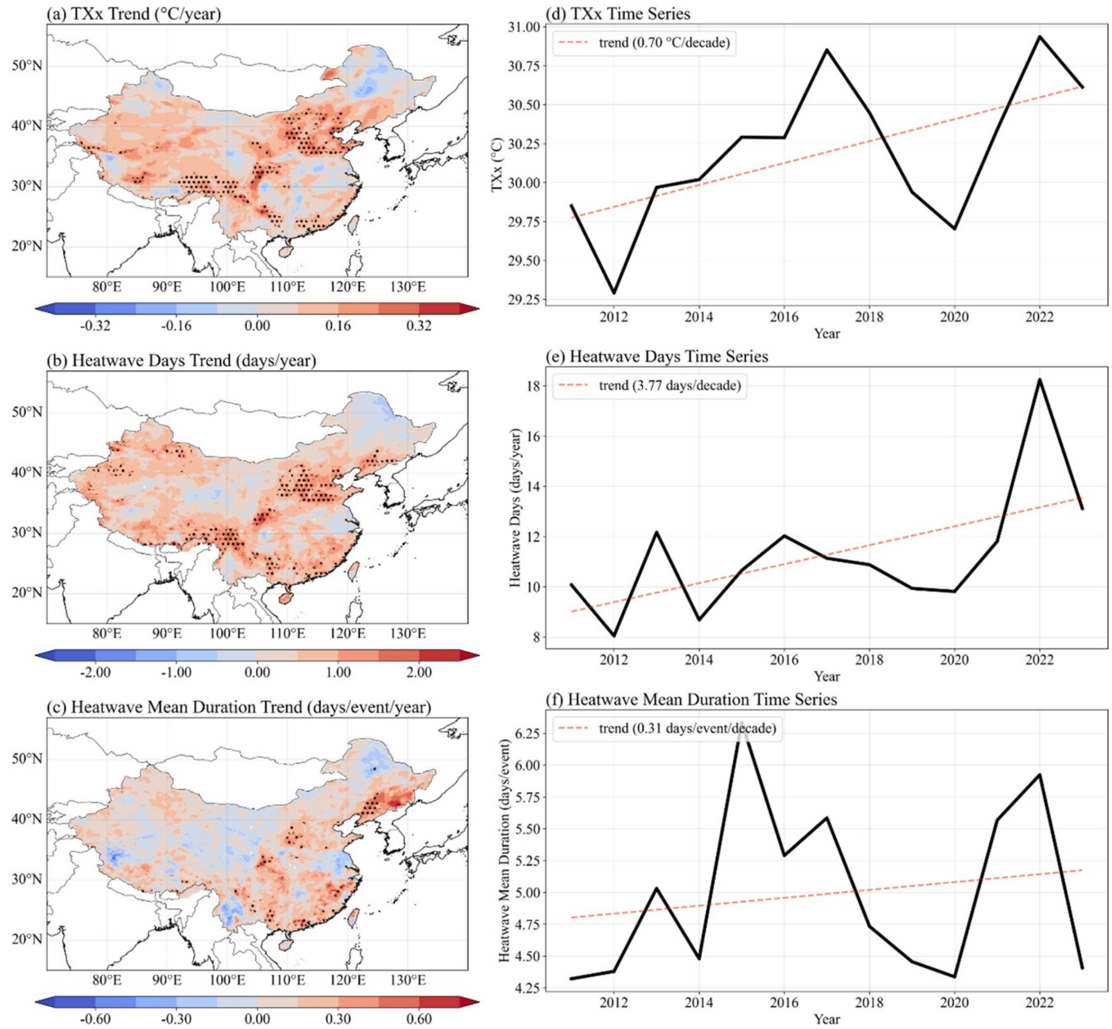

Figure 1. Linear trends in heat extreme indices in China from ERA5 reanalysis data. Spatial distribution of linear trends of (a) TXx (°C, the highest Tmax of the year for each grid), (b) heatwave days (days/year), and (c) heatwave mean duration (days/event) in the warm season (May–September) in China during 2011–2023. Time series (solid lines) of (d) TXx (°C), (e) heatwave days (days/year), and (f) heatwave mean duration (days/event) in the warm season in China from 2011 to 2023, with dashed lines representing the linear fitted trends. The shaded areas in a, b and c denote statistically significant at the 95% confidence level using the Student's *t* test.

of 0.2 ± 0.05 d/event. It suggests that the increase in CO_2 concentration contributed 43 ± 3% to the 0.7 °C/decade of the observed increasing trend of TXx in China during 2011–2023, as well as 27 ± 5% and 65 ± 16% of the increases in heatwave frequency and heat wave mean duration, respectively, due to their positive correlation with CO_2 concentrations.

The AOD in China shows a significant decline from 2011 to 2023, at a rate of –0.054 per decade. The reduction is largely attributed to the implementation of China's clean air policies, which have effectively curbed aerosol pollution. Based on the relationships between heat extreme indices and AOD derived from the 'hist-aer' experiment (figures 2(a)–(c)), the decline in AOD contributed approximately 27 ± 3% to the observed TXx trend during 2011–2023, as well as 15 ± 3% and 37 ± 7% of the increasing heatwave frequency and heatwave mean duration, respectively. These findings suggest that while CO_2 concentrations remain the dominant driver of heat extreme temperature increases, the reduction in aerosols from air quality improvements has also played a significant role in the intensifying heat extremes.

Aerosols affect surface temperature by directly scattering and absorbing sunlight, which reduces solar radiation reaching the surface (aerosol-radiation interaction), and indirectly by changing cloud properties, leading to more, smaller droplets that brighten clouds and increase cloud cover, thus cooling the surface (aerosol-cloud interaction) (Twomey 1974, Albrecht 1989, Luo *et al* 2020a, Huusko *et al* 2022). GHGs like CO_2 mainly warm the surface by trapping outgoing longwave radiation, enhancing the greenhouse effect (Ramanathan *et al* 1985, Chen and Dong 2019, Raghuraman *et al* 2023). Therefore, decreases in aerosols reduce their cooling effect, while rising CO_2 concentration increases warming, together influencing extreme heat events. The reduction in aerosols due to clean air actions leads to decreases in AOD and cloud

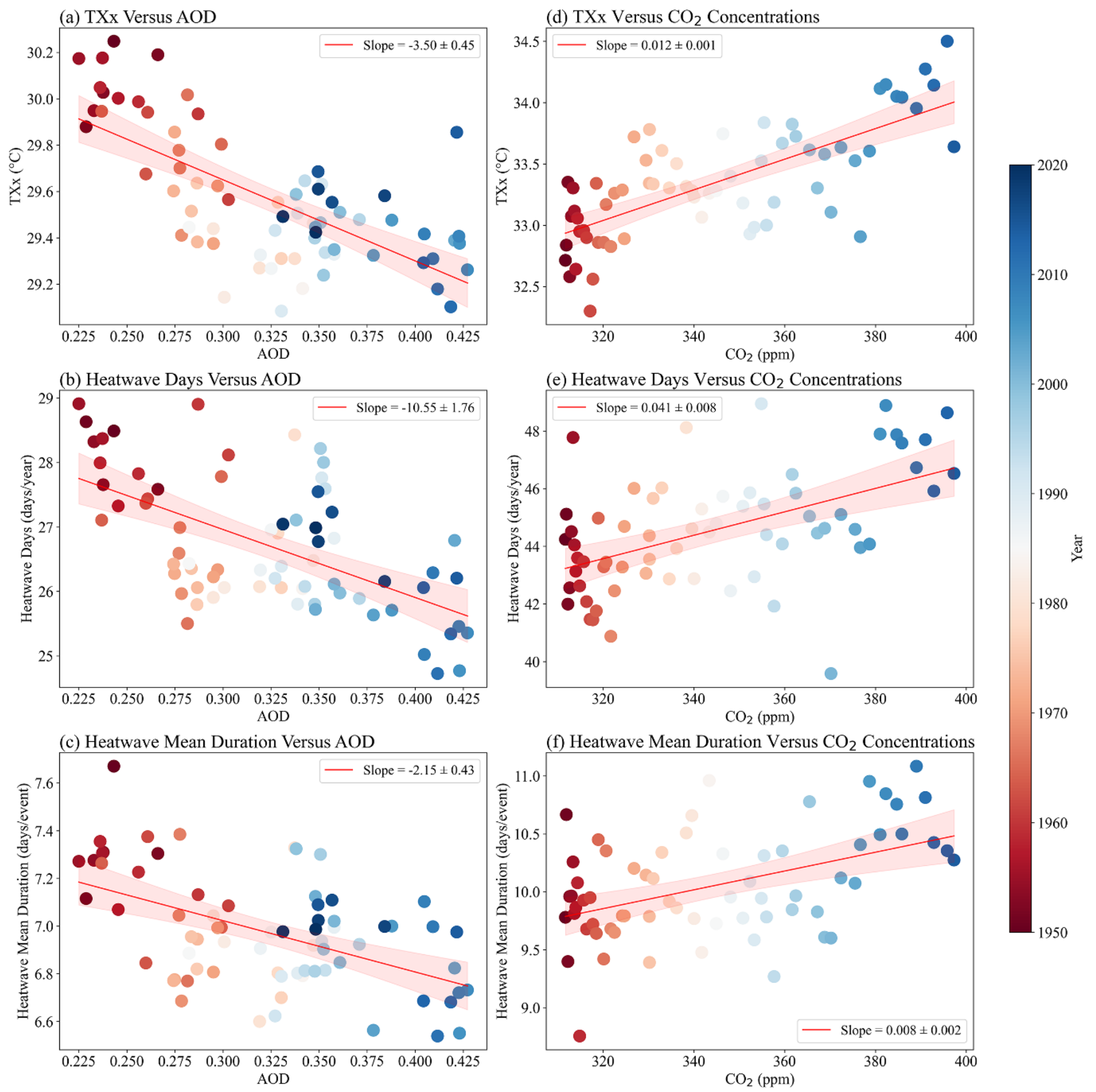

Figure 2. Relationships between heat extreme indices and AOD (unitless) or CO_2 concentrations (ppm) in China. Scatter plot of multi-model ensemble mean (a) TXx (°C), (b) heatwave days (days/year), and (c) heatwave mean duration (days/event) versus AOD in the warm season during 1950–2020 from the CMIP6-DAMIP 'hist-aer' experiment. Scatter plot of multi-model ensemble mean (d) TXx (°C), (e) heatwave days (days/year), and (f) heatwave mean duration (days/event) from the CMIP6-DAMIP 'hist-CO_2' experiment versus CO_2 concentrations from input4mips data in the warm season during 1950–2014. Lines represent the slope of linear fitting with standard errors, and the 95% confidence intervals are shown as shaded areas. The p-values of all fitted relationships are less than 0.01.

droplet number concentration (CDNC), which through aerosol-radiation and aerosol-cloud interactions cause a significant increase in the top-of-atmosphere (TOA) net downward radiative flux (figures 4(a)–(c)). It indicates that more radiation reaches the Earth, enhancing warming and intensifying extreme heat events in China. At the same time, the sustained increase in CO_2 concentration primarily enhances the absorption of longwave radiation emitted from the surface, resulting in an increase in TOA net downward radiative flux and thereby generating a greenhouse effect (figure 4(d)). This process is mainly driven by radiative forcing, but the associated warming may induce cloud feedbacks that moderately modulate the net radiative effect. Together, aerosol reductions and rising CO_2 concentrations act through distinct radiative mechanisms to jointly drive increases in the frequency, intensity, and duration of extreme high-temperature events.

Regional attributions in eastern China (east of 105°E) are also examined here, considering that this region not only experienced the high levels of aerosol loading but also exhibited the rapid decline in AOD across China since 2011 (figure S3). From 2011 to 2023, AOD in eastern China decreased at a rate of −0.13 per decade, while TXx, heatwave frequency, and heatwave mean duration increased

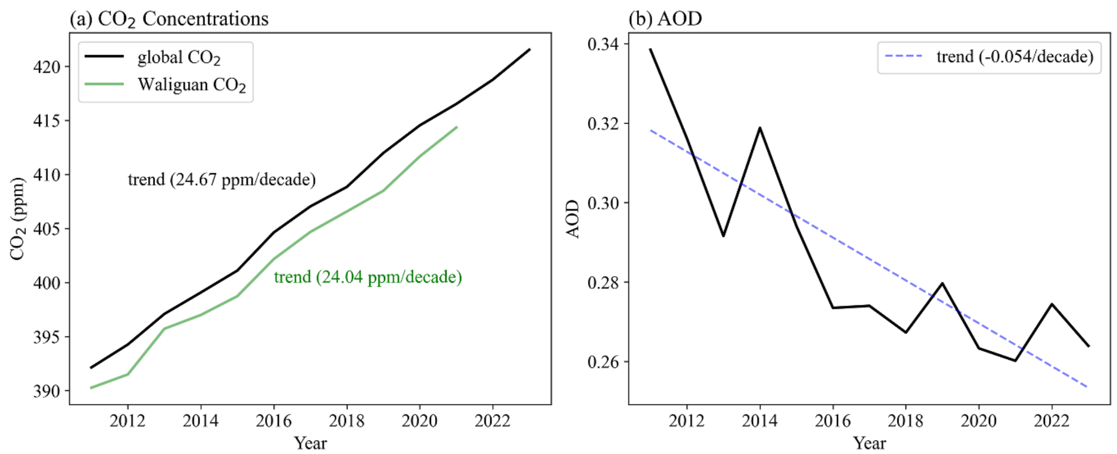

Figure 3. CO_2 concentrations (ppm) and AOD (unitless) trends in China. (a) Time series of global CO_2 concentrations from NOAA GML during 2011–2023 (black line) and CO_2 concentrations at the Waliguan station during 2011–2021 (green line). (b) Time series of regionally averaged warm season mean AOD in China from MERRA-2 reanalysis during 2011–2023, with dashed lines representing the linearly fitted trends.

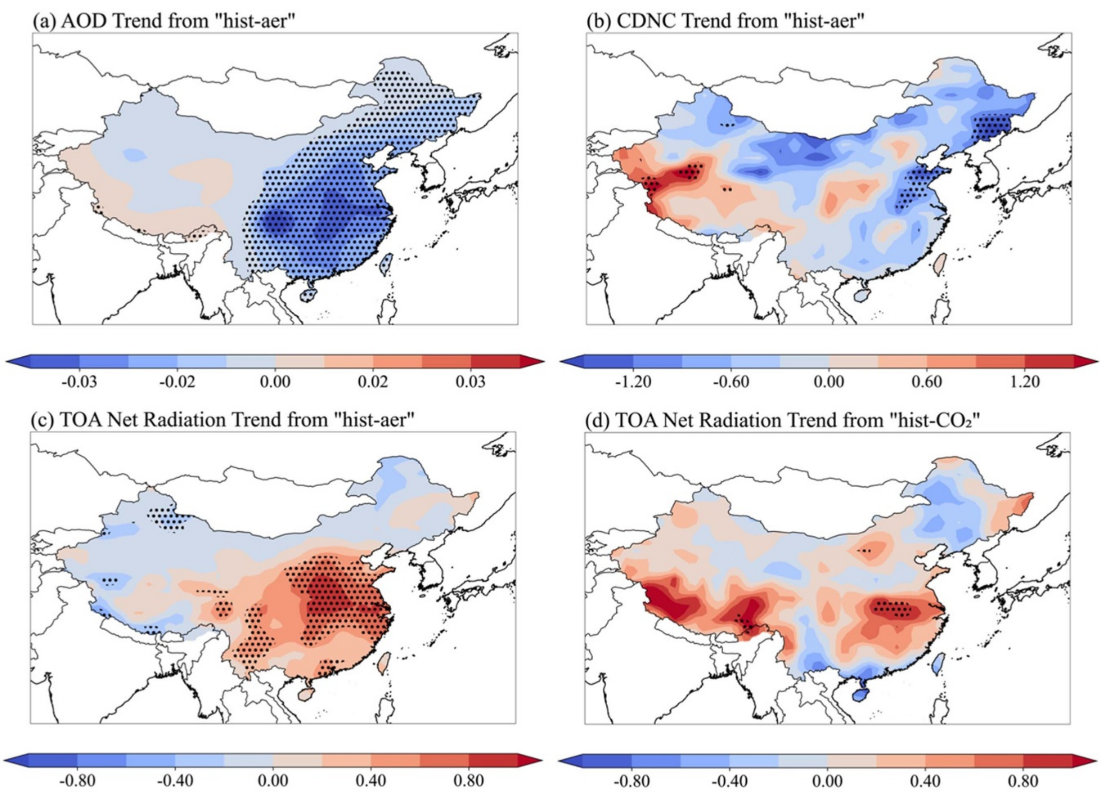

Figure 4. Linear trends in key variables related to aerosol and CO_2 forcing in China from CMIP6-DAMIP. Spatial distribution of trends in multi-model ensemble mean (a) AOD (/year), (b) CDNC (cm^{-3} yr^{-1}), (c) TOA net downward radiative flux ($W\ m^{-2}\ yr^{-1}$) from the CMIP6-DAMIP 'hist-aer' experiment, and (d) TOA net downward radiative flux ($W\ m^{-2}\ yr^{-1}$) from the CMIP6-DAMIP 'hist-CO_2' experiment in China during 2010–2020, with shaded areas representing statistically significant at the 95% confidence level using the Student's *t* test.

at a rate of 0.58 °C/decade, 3.41 d/decade and 0.64 d/event/decade, respectively (figure 5). The reductions in AOD contributed 79 ± 10% to the observed trend in TXx, 40 ± 7% to the trend in heatwave frequency, and 44 ± 9% to the trend in heatwave mean duration. In contrast, the increase in CO_2 concentrations contributed approximately 52 ± 3% to the TXx trend, 30 ± 6% to the heatwave

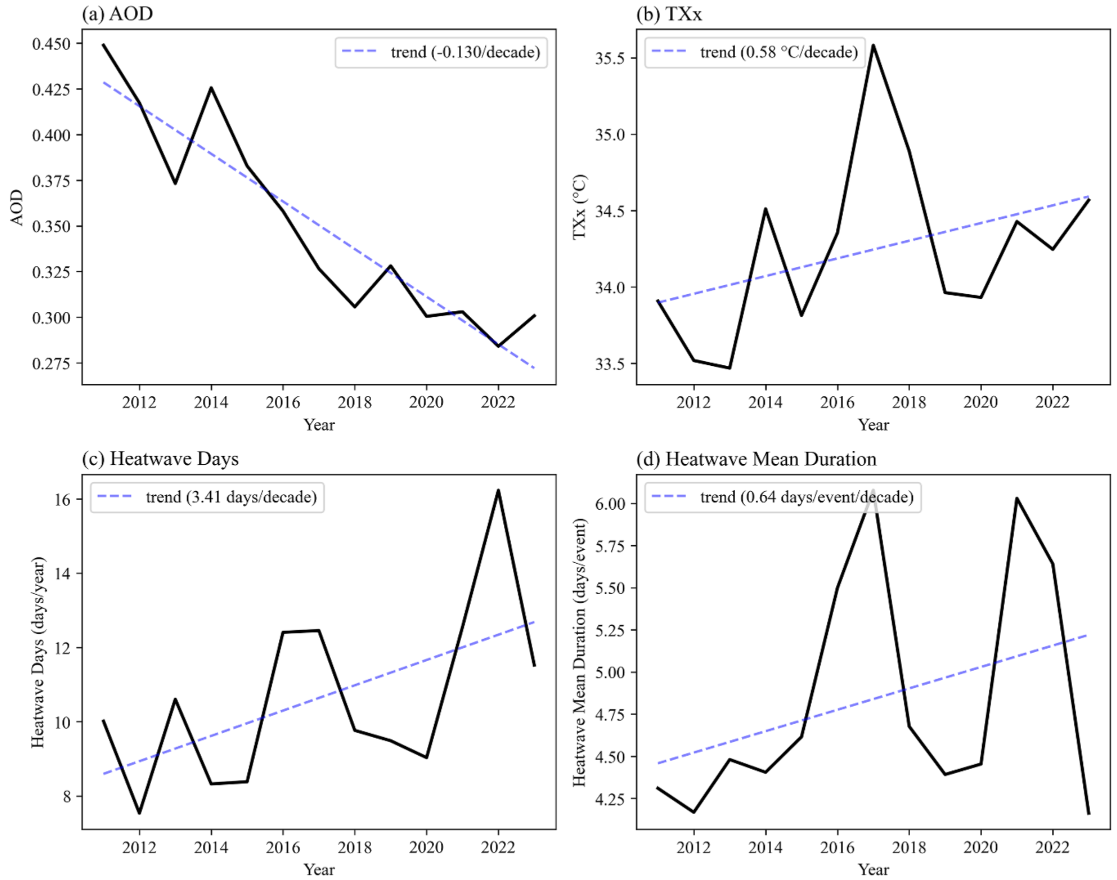

Figure 5. Linear trends in MERRA-2 AOD and heat extreme indices from ERA5 reanalysis data over eastern China (east of 105° E). Time series of regional averaged (a) mean AOD (unitless), (b) TXx (°C), (c) heatwave days (days/year), and (d) heatwave mean duration (days/event) over eastern China during the warm season from 2011 to 2023, with dashed lines representing the linearly fitted trends.

frequency trend, and 31 ± 8% to the heatwave mean duration trend. The results show a critical role of aerosol reductions played in driving the observed changes in extreme heat events in eastern China, contributing to higher intensity, more frequency, and longer duration of heatwaves.

4. Conclusions and discussions

This study reveals a significant intensification of heat extreme events across China during the warm season (May–September) from 2011 to 2023, characterized by rising maximum temperatures as well as more frequent and endured heatwave events. The core motivation of our study is to quantify the impact of the substantial decline in aerosol emissions in China since 2010s on the intensification of heat extremes, and to assess the relative contributions of aerosol reductions and rising GHGs to this recent trend, a dimension not explicitly addressed in previous literatures. The observed increasing trends in heat extreme indices, particularly TXx, heatwave frequency, and heatwave mean duration, are consistent with the broader patterns of global warming, driven primarily by the increasing concentrations of GHGs and decreasing aerosols. Our analysis shows that the rise in CO_2 level has exerted a profound influence on these heat extreme indices, contributing 43 ± 3%, 27 ± 5% and 65 ± 16% to the observed increasing trends in TXx, heatwave frequency and heatwave mean duration, respectively. The reduction in aerosols contributed approximately 27 ± 3% to the observed warming in TXx, 15 ± 3% to the increasing heatwave frequency, and 37 ± 7% to the prolonged heatwave duration from 2011 to 2023. Aerosol reductions decrease AOD and CDNC, enhancing TOA net downward radiative flux via aerosol-radiation and aerosol-cloud interactions, while rising CO_2 increases longwave radiation absorption, strengthening the greenhouse effect. In eastern China, the impacts of aerosol reductions were even more pronounced, with the reduction of AOD accounting for 79 ± 10% of the warming trend in TXx, 40 ± 7% of the increase in heatwave frequency, and 44 ± 9% of the rise in heatwave mean duration, which surpass the contributions of CO_2, especially in terms of maximum temperatures and the heatwave frequency. It suggests that air quality improvements, while being beneficial to public health, may have unintended consequences for climate extremes, particularly in a warming world.

In conclusion, while efforts of reducing CO_2 emissions are critical to addressing the climate change, strategies to manage aerosol concentrations also hold significant implications for mitigating heat extreme events. As China continues to combat air pollution, the trade-off between improving air quality and mitigating climate extremes must be carefully considered, especially in regions experiencing substantial aerosol reductions. Further research is needed to refine the understanding of these interactions and to explore effective strategies for minimizing the impacts of both aerosols and GHGs on heat extreme events in the future.

Data availability statement

The data that support the findings of this study are openly available at the following URL/DOI: https://doi.org/10.5281/zenodo.15172975 (Yang 2025).

Acknowledgments

This study was supported by the National Natural Science Foundation of China (Grant 42475032 and 42521006) and Jiangsu Innovation and Entrepreneurship Team (Grant JSSCTD202346). The Pacific Northwest National Laboratory (PNNL) is operated for DOE by the Battelle Memorial Institute under Contract DE-AC05-76RLO1830.

ORCID iDs

Aili Zou 0009-0004-9201-289X
Yang Yang 0000-0002-9008-5137
Ke Li 0000-0002-9181-3562
Hong Liao 0000-0001-6628-1798

References

Albrecht B A 1989 Aerosols, cloud microphysics, and fractional cloudiness *Science* **245** 1227–30

Ali M A *et al* 2022 Evaluation and comparison of CMIP6 models and MERRA-2 reanalysis AOD against satellite observations from 2000 to 2014 over China *Geosci. Front.* **13** 101325

Angélil O, Stone D A, Tadross M, Tummon F, Wehner M and Knutti R 2014 Attribution of extreme weather to anthropogenic greenhouse gas emissions: sensitivity to spatial and temporal scales *Geophys. Res. Lett.* **41** 2150–5

Bartusek S, Kornhuber K and Ting M 2022 2021 North American heatwave amplified by climate change-driven nonlinear interactions *Nat. Clim. Change* **12** 1143–50

Bellouin N *et al* 2020 Bounding global aerosol radiative forcing of climate change *Rev. Geophys.* **58** e2019RG000660

Benas N, Meirink J F, Karlsson K G, Stengel M and Stammes P 2020 Satellite observations of aerosols and clouds over southern China from 2006 to 2015: analysis of changes and possible interaction mechanisms *Atmos. Chem. Phys.* **20** 457–74

Bindoff N L, Stott P A, AchutaRao K M, Allen M R, Gillett N, Gutzler D and Zhang R 2014 Detection and attribution of climate change: from global to regional. Climate change 2013: the physical science basis (available at: https://hal.science/hal-03330685v1)

Boucher O, Kinne S and Cook J 2013 Aerosols, clouds, and climate change *Climate Change 2013: The Physical Science Basis, Intergovernmental Panel on Climate Change (IPCC)* (Cambridge University Press) pp 571–658

Chen W and Dong B 2019 Anthropogenic impacts on recent decadal change in temperature extremes over China: relative roles of greenhouse gases and anthropogenic aerosols *Clim. Dyn.* **52** 3643–60

Chen W, Dong B, Wilcox L, Luo F, Dunstone N and Highwood E J 2019 Attribution of recent trends in temperature extremes over China: role of changes in anthropogenic aerosol emissions over Asia *J. Clim.* **32** 7539–60

de Leeuw G, Kang H, Fan C, Li Z, Fang C and Zhang Y 2023 Meteorological and anthropogenic contributions to changes in the aerosol optical depth (AOD) over China during the last decade *Atmos. Environ.* **301** 119676

Dileepkumar R, AchutaRao K and Arulalan T 2018 Human influence on sub-regional surface air temperature change over India *Sci. Rep.* **8** 8967

Dong T, Zhu X, Deng R, Ma Y and Dong W 2022 Detection and attribution of extreme precipitation events over the Asian monsoon region *Weather Clim. Extremes* **38** 100497

Eyring V, Bony S, Meehl G A, Senior C A, Stevens B, Stouffer R J and Taylor K E 2016 Overview of the coupled model intercomparison project phase 6 (CMIP6) experimental design and organization *Geosci. Model Dev.* **9** 1937–58

Gillett N P, Shiogama H, Funke B, Hegerl G, Knutti R, Matthes K, Santer B D, Stone D and Tebaldi C 2016 The detection and attribution model intercomparison project (DAMIP v1. 0) contribution to CMIP6 *Geosci. Model Dev.* **9** 3685–97

Huusko L, Modak A and Mauritsen T 2022 Stronger response to the aerosol indirect effect due to cooling in remote regions *Geophys. Res. Lett.* **49** e2022GL101184

Iles C E, Samset B H, Sandstad M, Schuhen N, Wilcox L J and Lund M T 2024 Strong regional trends in extreme weather over the next two decades under high-and low-emissions pathways *Nat. Geosci.* **17** 1–6

IPCC 2021 Climate change 2021: the physical science basis *Working Group I Contribution to the IPCC Sixth Assessment Report*

Jia H, Ma X, Yu F and Quaas J 2021 Significant underestimation of radiative forcing by aerosol–cloud interactions derived from satellite-based methods *Nat. Commun.* **12** 3649

Jiang M, Li Y, Hu W, Yang Y, Brasseur G and Zhao X 2023 Model-based insights into aerosol perturbation on pristine continental convective precipitation *Atmos. Chem. Phys.* **23** 4545–57

Jones G S, Stott P A and Mitchell J F 2016 Uncertainties in the attribution of greenhouse gas warming and implications for climate prediction *J. Geophys. Res.* **121** 6969–92

Keeling C D, Bacastow R B, Bainbridge A E, Ekdahl C A Jr, Guenther P R, Waterman L S and Chin J F 1976 Atmospheric carbon dioxide variations at Mauna Loa observatory, Hawaii *Tellus* **28** 538–51

Kong Z, Cao J and Wang B 2025 Anthropogenic aerosol dominates the decadal change in evapotranspiration over southeastern China in the past four decades *Remote Sens.* **17** 561

Kweku D W, Bismark O, Maxwell A, Desmond K A, Danso K B, Oti-Mensah E A, Quachie A T and Adormaa B B 2018

Greenhouse effect: greenhouse gases and their impact on global warming *J. Sci. Res. Rep.* **17** 1–9
Li X X, Yuan C and Hang J 2022 Heat wave trends in Southeast Asia: comparison of results from observation and reanalysis data *Geophys. Res. Lett.* **49** e2021GL097151
Li X, Liu Y, Wang M, Jiang Y and Dong X 2021 Assessment of the coupled model intercomparison project phase 6 (CMIP6) model performance in simulating the spatial-temporal variation of aerosol optical depth over Eastern central China *Atmos. Res.* **261** 105747
Liang M, Han Z, Li J, Li Y and Liang L 2024 Aerosol effects during heat waves in summer 2022 and responses to emission change over China *npj Clim. Atmos. Sci.* **7** 190
Luo F, Wilcox L, Dong B, Su Q, Chen W, Dunstone N, Li S and Gao Y 2020a Projected near-term changes of temperature extremes in Europe and China under different aerosol emissions *Environ. Res. Lett.* **15** 034013
Luo M, Ning G, Xu F, Wang S, Liu Z and Yang Y 2020b Observed heatwave changes in arid northwest China: physical mechanism and long-term trend *Atmos. Res.* **242** 105009
Ma J *et al* 2020 MAX-DOAS measurements of NO_2, SO_2, HCHO, and BrO at the Mt. Waliguan WMO GAW global baseline station in the Tibetan Plateau *Atmos. Chem. Phys.* **20** 6973–90
Perkins-Kirkpatrick S E and Lewis S C 2020 Increasing trends in regional heatwaves *Nat. Commun.* **11** 3357
Qi C, Wang P, Yang Y, Li H, Zhang H, Ren L, Jin X, Zhan C, Tang J and Liao H 2024 Impacts of tropical cyclone–heat wave compound events on surface ozone in eastern China: comparison between the Yangtze River and Pearl River deltas *Atmos. Chem. Phys.* **24** 11775–89
Raghuraman S P, Paynter D, Ramaswamy V, Menzel R and Huang X 2023 Greenhouse gas forcing and climate feedback signatures identified in hyperspectral infrared satellite observations *Geophys. Res. Lett.* **50** e2023GL103947
Ramanathan V, Cicerone R J, Singh H B and Kiehl J T 1985 Trace gas trends and their potential role in climate change *J. Geophys. Res.* **90** 5547–66
Seong M, Min S, Kim Y, Zhang X and Sun Y 2021 Anthropogenic greenhouse gas and aerosol contributions to extreme temperature changes during 1951–2015 *J. Clim.* **34** 857–70
Seong M, Min S and Zhang X 2022 A Bayesian attribution analysis of extreme temperature changes at global and regional scales *J. Clim.* **35** 8189–203
Sharma A, Andhikaputra G and Wang Y C 2022 Heatwaves in South Asia: characterization, consequences on human health, and adaptation strategies *Atmosphere* **13** 734
Shilin A, Ghosh S and Karmakar S 2024 Flipping of temperature and precipitation trends over the Indian subcontinent due to diametrically opposing influence of GHGs and aerosols *Environ. Res. Lett.* **19** 064045
Singh S, Mall R K and Singh N 2021 Changing spatio-temporal trends of heat wave and severe heat wave events over India: an emerging health hazard *Int. J. Climatol.* **41** 1831–45
Sonali P and Nagesh Kumar D 2016 Detection and attribution of seasonal temperature changes in India with climate models in the CMIP5 archive *J. Water Clim. Change* **7** 83–102
Twomey S 1974 Pollution and the planetary albedo *Atmos. Environ.* **8** 1251–6
Wang J and Yan Z 2021 Rapid rises in the magnitude and risk of extreme regional heat wave events in China *Weather Clim. Extremes* **34** 100379
Wang P, Yang Y, Xue D, Qu Y, Tang J, Leung L R and Liao H 2023b Increasing compound hazards of tropical cyclones and heatwaves over southeastern coast of China under climate warming *J. Clim.* **36** 2243–57
Wang P, Yang Y, Xue D, Ren L, Tang J, Leung L R and Liao H 2023a Aerosols overtake greenhouse gases causing a warmer climate and more weather extremes toward carbon neutrality *Nat. Commun.* **14** 7257
Wang X, Jiang D and Lang X 2017 Future extreme climate changes linked to global warming intensity *Sci. Bull.* **62** 1673–80
Wei J, Wang W, Wang G, Cao M, Yang L, Zhang S, Fu J and Xing W 2023 Projecting the changes in multifaceted characteristics of heatwave events across China *Earth's Future* **11** e2022EF003387
Whan K, Zscheischler J, Orth R, Shongwe M, Rahimi M, Asare E O and Seneviratne S I 2015 Impact of soil moisture on extreme maximum temperatures in Europe *Weather Clim. Extremes* **9** 57–67
White R H *et al* 2023 The unprecedented Pacific northwest heatwave of June 2021 *Nat. Commun.* **14** 727
Xu W, Lin T, Lei X, Chen Y and Gao L 2023 Anthropogenic emissions and land use/cover change contributions to extreme temperature changes over China *Atmos. Res.* **292** 106845
Xu Y, Ramanathan V and Victor D G 2018 Global warming will happen faster than we think *Nature* **564** 30–32
Yang Y 2025 Data for "Intensifying heat extremes in China attributed to rising greenhouse gases and declining aerosols since the 2010s" *Zenodo* https://doi.org/10.5281/zenodo.15172975
Yang Y, Zeng L, Wang H, Wang P and Liao H 2023 Climate effects of future aerosol reductions for achieving carbon neutrality in China *Sci. Bull.* **68** 902–5
Ye F, Wang P, Yang Y, Ren L, Tang J and Liao H 2025 Anthropogenic forcing dominates changes in compound long-duration dry and heat extremes in China *Clim. Change* **178** 30
Zhang G, Zeng G, Iyakaremye V and You Q 2020 Regional changes in extreme heat events in China under stabilized 1.5 C and 2.0 C global warming *Adv. Clim. Change Res.* **11** 198–209
Zhang X, Huang T, Wang W and Shen P 2024 Change of global land extreme temperature in the future *Glob. Planet. Change* **242** 104583
Zhao A, Bollasina M A and Stevenson D S 2019 Strong influence of aerosol reductions on future heatwaves *Geophys. Res. Lett.* **46** 4913–23
Zhu H, Jiang Z and Li L 2021 Projection of climate extremes in China, an incremental exercise from CMIP5 to CMIP6 *Sci. Bull.* **66** 2528–37
Zou A, Yang Y, Wang H, Wang P and Liao H 2025 Aerosol decline accelerates the increasing extreme precipitation in China *Geophys. Res. Lett.* **52** e2024GL113887